Theoretical and Applied Climatology (2021) 145:925–939
https://doi.org/10.1007/s00704-021-03654-5

ORIGINAL PAPER

Calibration of empirical equations for estimating reference evapotranspiration in different climates of Iran

Saeed Sharafi[1] · Mehdi Mohammadi Ghaleni[2]

Received: 17 March 2021 / Accepted: 5 May 2021 / Published online: 8 June 2021

Abstract

The accurate estimation of reference evapotranspiration (ET_{ref}) is a crucial component for modeling hydrological and ecological cycles. The goal of this study was the calibration of 32 empirical equations used to determine ET_{ref} in the three classes of temperature-based, solar radiation–based, and mass transfer–based evapotranspiration. The calibration was based on measurements taken between the years 1990 and 2019 at 41 synoptic stations located in very dry, dry, semidry, and humid climates of Iran. The performance of the original and calibrated empirical equations compared to the PM-FAO_{56} equation was evaluated based on model evaluation techniques including the coefficient of determination (R^2), the root mean square error (RMSE), the average percentage error (APE), the mean bias error (MBE), the index of agreement (D), and the scatter index (SI). The results show that the calibrated Baier and Robertson equation for temperature-based models, the Jensen and Haise equation for solar radiation–based models, and the Penman equation for mass transfer–based models performed better than the original empirical equations. The calibrated equations had, respectively, an average $R^2 = 0.73$, 0.67, and 0.78; RMSE = 35.14, 35.02, and 30.20 mm year^{-1}; and MBE = − 5.6, − 3.89, and 2.57 mm year^{-1}. The original empirical equations had values of average $R^2 = 0.60$, 0.37, and 0.65; RMSE = 68.34, 66.98, and 52.62 mm year^{-1}; and MBE = − 5.75, 4.26, and 8.99 mm year^{-1}, respectively. The calibrated empirical equations for very dry climate (e.g., Zabol, Zahedan, Bam, Iranshahr, and Chabahar stations) also significantly reduced the SI value from SI > 0.3 (poor class) to SI < 0.1 (excellent class). Therefore, the calibrated empirical equations are highly recommended for estimating ET_{ref} in different climates.

Keywords Calibration · ET_{ref} estimation · Scatter index · Water resource · Zonation

1 Introduction

Water resources in semiarid regions are vulnerable to the impacts of climate change and human activities, and the accurate estimation of reference evapotranspiration (ET_{ref}) is a primary tool in the management of water resources. Also, the estimation of ET_{ref} by using hydrological equations can be helpful in agriculture sectors (Celestin et al. 2020; Ndiaye et al. 2020; Yan et al. 2021). It has a key role in the management of water resources and the determination of crops' water demands in the semidry regions (Berti et al. 2014; Ferreira et al. 2019; dos Santos Farias et al. 2020).

The most accurate evaluation of ET_{ref} is computed by the lysimeter method, but this method has high costs and requires complex instruments (Ahooghalandari et al. 2016; Ahooghalandari et al. 2017). Therefore, alternative techniques for indirect estimation of ET_{ref} were developed based on empirical equations. Numerous empirical equations have been introduced to estimate ET_{ref}. Despite the advantages of empirical equations such as ease of use, applicability due to the great variety of required parameters, and classification based on various climatic parameters, the low accuracy of some of these equations in estimating ET_{ref} is one of the main challenges in their application. In contrast, the FAO_{56} Penman-Monteith (PM-FAO_{56}) equation is the standard combination-based model used to estimate the ET_{ref} in different climates and at different time scales (Güçlü et al. 2017; Saggi and Jain 2019; Shiri et al. 2019; Ndiaye et al. 2020; Sharafi and Mohammadi Ghaleni 2021). The accuracy of this equation is due to its

✉ Saeed Sharafi
s-sharafi@araku.ac.ir

[1] Department of Environment Science and Engineering, Arak University, Arak, Iran

[2] Department of Water Science and Engineering, Arak University, Arak, Iran

consideration of all climatic parameters, including solar radiation, air temperature, wind speed, and relative humidity (Ndiaye et al. 2020). Furthermore, the equations for empirical models based on temperature, solar radiation, and mass transfer use fewer climatic parameters in the calculation of ET_{ref}. Therefore, the development and calibration of empirical model equations in different climates can be more effective for agricultural and hydrological projects where only a few climatic variables are available (Heydari and Heydari and Heydari 2014; Gafurov et al. 2018).

Several researchers have evaluated the dependence of different empirical ET_{ref} equations on various meteorological parameters over different climates. Gao et al. (2017) also assessed different empirical ET_{ref} equations in various climates and observed that the PT and Hargreaves (HG) equations worked best in dry and semidry climates, while the MK equation worked best in the humid climate of China. Sharafi and Ghaleni 2021) evaluated different empirical equations for ET_{ref} in different climates of Iran. Their results found that the simplest regression model (MLR) based on minimum and maximum temperature data was more precise than the empirical equations. They also recommended the solar radiation–based Irmak equation as the best substitute for the PM-FAO_{56} model, especially in dry and semidry climates.

Rahimikhoob et al. (2012) compared four temperature-based and solar radiation–based equations using data from eight stations in subtropical climates of Iran and confirmed the applicability of Priestley–Taylor (PT) and Hargreaves–Samani (HS) equations in those climates. The comparison results showed that the original PT and HS equations were more applicable in a humid climate. The performance of the PT and HS equations improved slightly after the calibration; however, the Trajkovic (TRAJ) and Makkink (MAKK) equations improved greatly. Tabari et al. (2013) compared different temperature-based, solar radiation–based, and mass transfer–based equations for modeling ET_{ref} in humid climates of Iran and found that the temperature-based Blaney–Criddle (BC) and HS equations surpassed the other temperature-based models. Cross-comparison of the 31 empirical equations showed that the five best equations as compared with the PM-FAO_{56} model were the two solar radiation–based equations developed, the temperature-based BC and Hargreves-M4 equations.

Farzanpour et al. (2019) conducted 20 ET_{ref} equations using daily meteorological data of 10 stations (12 years) in semidry climates of Iran. Their results revealed that the calibrated equations might be a good alternative for the PM-FAO_{56} equation. Bourletsikas et al. (2018) compared 24 different equations for estimating ET_{ref} in Greece and concluded that calibrating mass transfer-based equations is essential for improving their performances. Celestin et al. (2020) compared the 32 empirical ET_{ref} equations with the PM-FAO_{56} using data on temperature, solar radiation, and mass transfer in northwest China. They found that the World Meteorological Organization (WMO) and the Mahringer equations for the mass transfer–based model provided the best results.

Above all, in the present study, we have tried to introduce the best calibrated equations with the highest accuracy in different climates of Iran. Therefore, the goals of this study were (1) the use of monthly data of eight climatic variables measured in 41 synoptic stations over a period of 30 years (1990–2019); (2) the calibration of 32 empirical equations based on temperature-based, solar radiation–based, and mass transfer–based equations in four main climates (very dry, dry, semidry, and humid) in the study area; (3) the comparison of the results of the original and calibrated equations versus the PM-FAO_{56} equation using different statistical criteria; and (4) drawing an accurate map of the results of the best calibrated empirical equations in the study area.

2 Materials and methods

2.1 Time and location scales

Iran is in the northern hemisphere between 25 and 40° latitude. For this study, meteorological data recorded between 1990 and 2019 were collected from 41 synoptic stations in the country. These data were collected by the National Meteorological Organization of Iran and include the monthly mean of minimum, mean and maximum air temperature, relative humidity, wind speed measured at 2 m height, and solar radiation. The data were complete, and no data needed to be reconstructed.

According to the FAO_{56} index, Iran is classified into four climatic regions: very dry, dry, semidry, and humid (Fig. 1). Figure 1 shows the location and climate for each station used in this study. Six stations were in very dry climate, 17 stations in dry climate, 14 stations in semidry climate, and 4 stations in humid climate (Fig. 1).

2.2 Empirical ET_{ref} equations

Based on the type and importance of input variables used in each empirical equation to calculate the ET_{ref}, the models were divided into 4 categories: combination-based (1 equation), temperature-based (11 equations), solar radiation–based (11 equations), and mass transfer–based (10 equations). Table 1 lists the 33 empirical ET_{ref} equations used in this study and their respective references.

To calculate the PM-FAO_{56}, measurements of the amount of total solar radiation at the Earth's surface (R_s, MJ m^{-2} d^{-1}), maximum and minimum temperature, wind speed (m s^{-1}), and lack of vapor pressure (VPD, kPa) are required. Due to lack of access to R_s and VPD, the FAO method was used (Gholipoor 2009). Daily values of R_s were obtained from Hargreaves and

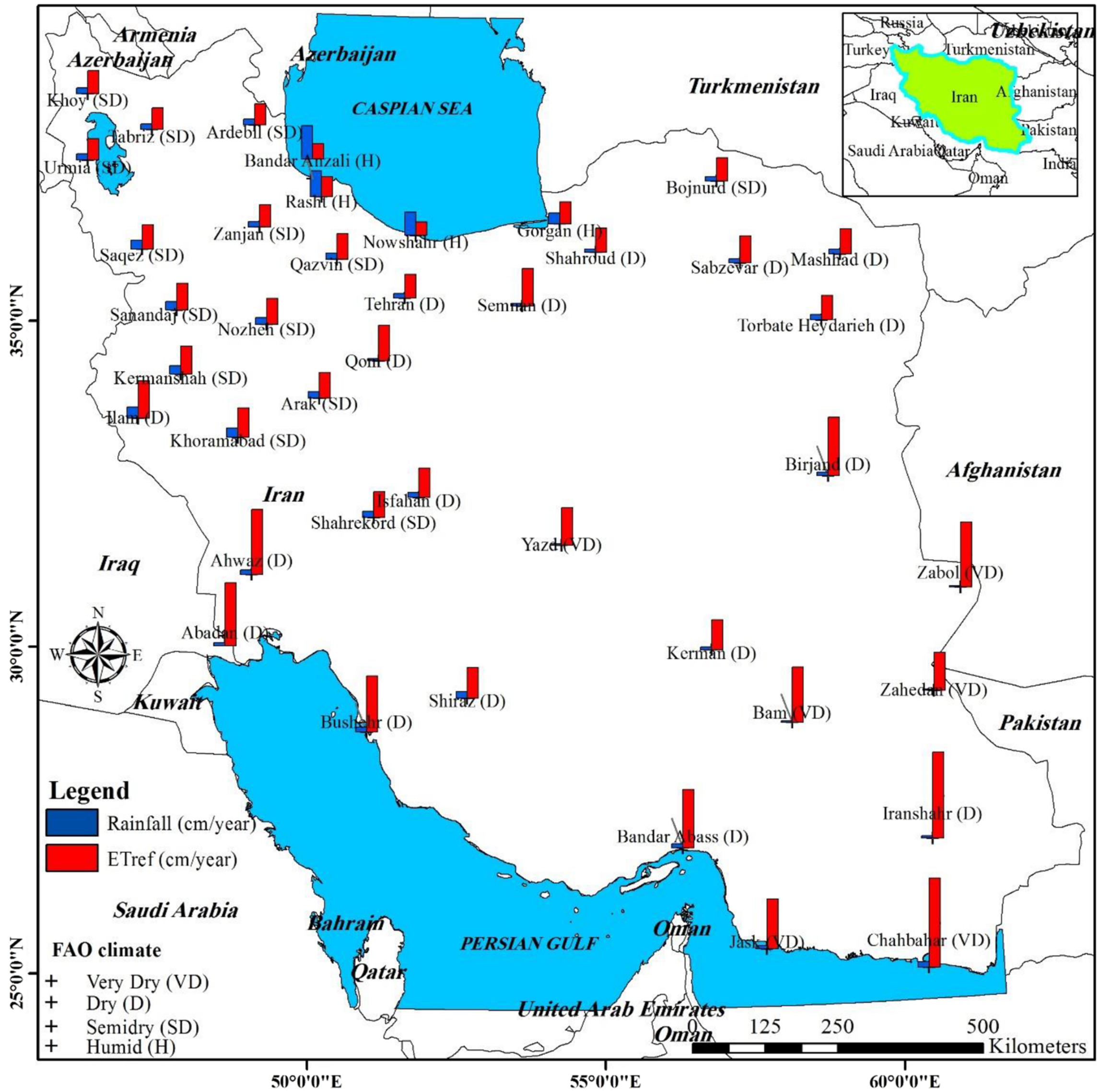

Fig. 1 Location and classification of studied stations based on the FAO_{56} method

Samani's equation (Mehdizadeh et al. 2017) and the modified Allen et al. (2006) equation. Solar radiation reaching the land surface (R_n, MJ m^{-2} d^{-1}) was first measured above the Earth's atmosphere for each day of the year based on latitude and longitude and the solar constant (Allen et al. 2006). Then, R_s was calculated using Eq. 34:

$$Rs = K_{Rs} \times \left(1 + 2.7 \times 10^{-5} \times Alt\right) \times \left(T_{\max} - T_{\min}\right)^{0.5} \times R_n \quad (34)$$

where Alt is altitude (m) and K_{Rs} is the empirical constant, considered equal to 0.16 (Gholipoor 2009). The e_s calculation is obtained from the difference between the daily saturated water vapor pressure (e_{max}) and the actual water vapor pressure (e_a). Relative humidity at temperature was assumed to be at least 100 percent and the values for e_a were obtained from Eq. (35):

$$e_a = 0.6108 \times \exp\frac{(17.27 \times T_{\min})}{(T_{\min} + 237.3)} \quad (35)$$

In very dry and dry climates, the relative humidity at the T_{min} may never reach 100%. Therefore, it was assumed that in these regions, e_a values would occur at $T_{min} > 10$ °C and it was observed that in this case it had a minor effect on ET_{ref} (1–2%). As a result, the ET_{ref} was calculated assuming that the dew point was equal to the T_{min}. Then, the T_{max} saturated vapor pressure during the day (e_{max}) depending on the T_{max} was obtained from Eq. (36).

$$e_{\max} = 0.6108 \times \exp\frac{(17.27 \times T_{\max})}{(T_{\max} + 237.3)} \quad (36)$$

Table 1 The ET_{ref} estimated based on empirical equations

Code	Abs.	Empirical equations	References
Combination-based			
1	PM-FAO$_{56}$	$ET_{ref} = 0.408\Delta(R_n - G)\frac{+\gamma[900/(T_{mean}+273)]u_2(e_s-e_a)}{\Delta+\gamma(1+0.34u_2)}$	Allen et al. (2006)
Temperature-based			
2	HASA	$ET_{ref}=[0.0023\times R_a(T_{mean}+17.8)(T_{\max}-T_{\min})^{0.5}]/\lambda$	Hargreaves and Samani (1985)
3	TRAJ	$ET_{ref}=[0.0023\times R_a(T_{mean}+17.8)(T_{\max}-T_{\min})^{0.424}]/\lambda$	Trajkovic (2007)
4	TATA1	$ET_{ref}=[0.0031\times R_a(T_{mean}+17.8)(T_{\max}-T_{\min})^{0.5}]/\lambda$	Tabari and Talaee (2011)
5	TATA2	$ET_{ref}=[0.0028\times R_a(T_{mean}+17.8)(T_{\max}-T_{\min})^{0.5}]/\lambda$	Tabari and Talaee (2011)
6	DRAL1	$ET_{ref}=[0.003\times R_a(T_{mean}+20)(T_{\max}-T_{\min})^{0.4}]/\lambda$	Droogers and Allen (2002)
7	DRAL2	$ET_{ref}=[0.0025\times R_a(T_{mean}+16.8)(T_{\max}-T_{\min})^{0.5}]/\lambda$	Droogers and Allen (2002)
8	BERT	$ET_{ref}=[0.00193\times R_a(T_{mean}+17.8)(T_{\max}-T_{\min})^{0.517}]/\lambda$	Berti et al. (2014)
9	DORJ	$ET_{ref}=[0.002\times R_a(T_{mean}+33.9)(T_{\max}-T_{\min})^{0.296}]/\lambda$	Dorji et al. (2016)
10	BARO	$ET_{ref}=0.109\times(R_a/\lambda)+0.157T_{\max}+0.158(T_{\max}-T_{\min})-5.39$	Baier and Robertson (1965)
11	AHOO1	$ET_{ref}=0.252\times(R_a/\lambda)+0.221T_{mean}(1-RH/100)$	Ahooghalandari et al. (2016)
12	AHOO2	$ET_{ref}=0.29\times(R_a/\lambda)+0.15T_{\max}(1-RH/100)$	Ahooghalandari et al. (2016)
Solar radiation–based			
13	MAKK	$ET_{ref}=0.7\times(R_a/\lambda)\times[\Delta/\Delta+\gamma]-0.12$	Makkink (1957)
14	PRTA	$ET_{ref}=1.26\times(R_n-G)[\Delta/\Delta+\gamma]/\lambda$	Priestley and Taylor (1972)
15	JEHA	$ET_{ref}=(0.025T_{mean}+0.08)R_s/\lambda$	Jensen and Haise (1963)
16	HARG	$ET_{ref}=[0.0135(T_{mean}+17.8)R_s]/\lambda$	Hargreaves (1975)
17	ABTE1	$ET_{ref}=0.25T_{\max}R_s/\lambda$	Abtew (1996)
18	ABTE2	$ET_{ref}=(T_{\max}/56)\times(R_s/\lambda)$	Abtew (1996)
19	IRMA1	$ET_{ref}=-0.611+0.149R_s+0.079T_{mean}$	Irmak et al. (2003)
20	IRMA2	$ET_{ref}=0.469+0.289R_n+0.023T_{mean}$	Irmak et al. (2003)
21	TATA3	$ET_{ref}=-0.642+0.174R_s+0.0353T_{mean}$	Tabari and Talaee (2011)
22	TATA4	$ET_{ref}=-0.478+0.156R_s-0.0112T_{\max}+0.0733T_{\min}$	Tabari and Talaee (2011)
23	OUDI	$ET_{ref}=(R_s/\lambda)\times[T_{mean}+5]/100$	Oudin (2004)
Mass transfer–based			
24	DALT	$ET_{ref}=(3.648+0.7223u_2)(e_s-e_a)$	Dalton (1802)
25	MEYE	$ET_{ref}=(3.75+0.503u_2)(e_s-e_a)$	Meyer (1926)
26	ROHW	$ET_{ref}=(3.3+0.891u_2)(e_s-e_a)$	Rohwer (1931)
27	ALBR	$ET_{ref}=(1.005+2.97u_2)(e_s-e_a)$	Albrecht (1950)
28	WMO	$ET_{ref}=(1.298+0.934u_2)(e_s-e_a)$	WMO (1966)
29	TRAB	$ET_{ref}=0.3075\times u_2^{0.5}(e_s-e_a)$	Trabert (1896)
30	BRWE	$ET_{ref}=0.543\times u_2^{0.456}(e_s-e_a)$	Brockamp and Wenner (1963)
31	MAHR	$ET_{ref}=0.286\times u_2^{0.5}(e_s-e_a)$	Mahringer (1970)
32	PENM	$ET_{ref}=(2.625+0.000479u_2)(e_s-e_a)$	Penman (1948)
33	ROMA	$ET_{ref}=0.00006(100-RH)(25+T_{mean})^2$	Romanenko (1961)

ET_{ref} reference evapotranspiration (mm day^{-1}); Δ the slope of saturation vapor pressure curve (mb $^{\circ}$C^{-1}); Rn net solar radiation (MJ m^{-2} day^{-1}); G soil heat flux density (mm day^{-1}); γ psychometric constant (kPa $^{\circ}$C^{-1}); $T_{mean,\ max\ and\ min}$ mean, maximum, and minimum daily temperature (°C), respectively; u_2 wind speed measured at 2 m height (m s^{-1}); R_a extraterrestrial radiation (mm day^{-1}); λ latent heat of vaporization (MJ kg^{-1}); RH mean relative humidity (%); R_s solar radiation (MJ m^{-2} day^{-1}); e_s saturation vapor pressure (k Pa); e_a actual vapor pressure (k Pa); and $(e_s$-$e_a)$ saturation vapor pressure deficit (kPa)

where e_s is obtained from the mean e_a and e_{max}. Finally, e_s is calculated as the average between e_a and e_{max} in a part of the day when the air temperature is not at its maximum. However, other researchers have found that $(e_{max}$-$e_a) \times 0.75$ is a more accurate estimate of e_a (Tanner and Sinclair 1983; Allen et al. 1998). Therefore, this method is used in this current study. Calculations were performed using SAS software (Statistical Analysis System, Version 9.1, SAS Inst., Cary, NC).

The average annual rainfall over the last 30 years in Iran was reported to be 334 mm. The highest annual rainfall occurred at Bandar Anzali station (1791.78 mm), and the lowest annual rainfall occurred at Bam station (61.61 mm). The average annual rainfall in the very dry climate was 92.89 mm, which was 140.74, 266.41, and 1150.05 mm less than in dry, semidry, and humid climates, respectively (Fig. 2(a)). The annual average relative humidity in Iran was reported to be 55.34% with the highest relative humidity at Bandar Anzali station (84.71%) and the lowest relative humidity at Bam station (28.08%). The relative humidity in the very dry climate was 44.64%, which was 1.02, 7.9, and 35.93% less than in the dry, semidry, and humid climates, respectively (Fig. 2(b)).

The 30-year average air temperature in Iran was reported to be 17.54 °C. The hottest and coldest stations in this study were the Bandar Abbas and Ardabil stations (26.63 and 9.14 °C, respectively). The average air temperature in the very dry climate was 20.44 °C, which was 3.4, 10.15, and 6.04 °C warmer than in the dry, semidry, and humid climates, respectively (Fig. 2(c)). The average solar radiation received in Iran is reported to be 7.26 MJ m^{-2} day^{-1}. The highest and lowest received solar radiations were observed in Bam and Rasht stations (9.06 and 4.17 MJ m^{-2} day^{-1}, respectively). The average solar radiation received in the very dry climate was 8.55 MJ m^{-2} day^{-1}, which increased by 0.36, 1.06, and 3.74 MJ m^{-2} day^{-1} in dry, semidry, and humid climates (Fig. 2(d)). The average wind speed in the country during the last 30 years was reported to be 4.35 m s^{-1}, which has increased by about 0.52 m s^{-1} compared to the same period. The highest and lowest wind speeds were recorded in Zabol and Gorgan stations, respectively (10.62 and 1.45 m s^{-1}). The mean wind speed in a very dry climate was 6.54 m s^{-1}, which increased by 2.15, 2.63, and 3.97 m s^{-1} in dry, semidry, and humid climates (Fig. 2(e)).

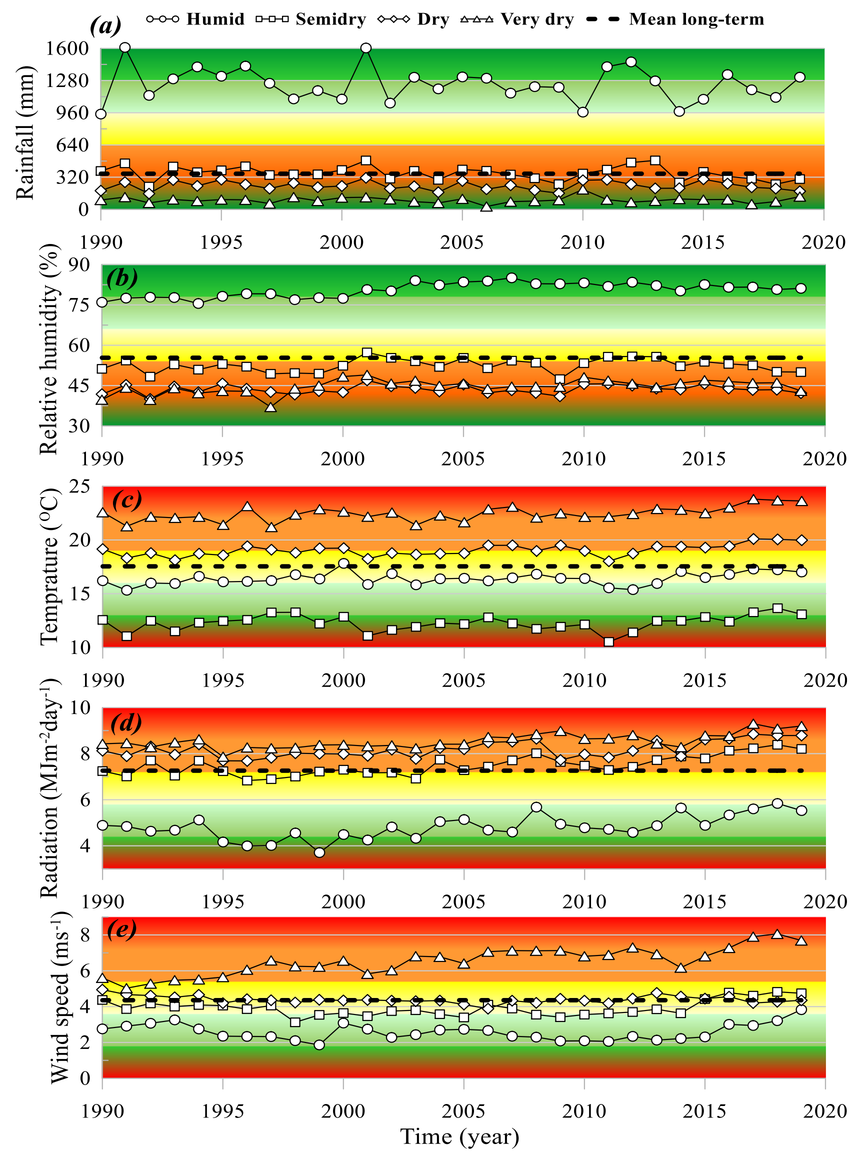

Fig. 2 The long period values of (**a**) rainfall, (**b**) relative humidity, (**c**) temperature, (**d**) solar radiation, and (**e**) wind speed of Iran's climate (1990–2019)

2.3 Evaluation performance criteria

Until now, many performance criteria have been used to evaluate the results of the model for prediction of ET_{ref}. The equations were assessed for each station by means of six statistical measures used to evaluate the accuracy of each model in estimating the ET_{ref}: the coefficient of determination (R^2), the root mean square error (RMSE), the average percentage error (APE), the mean bias error (MBE), the index of agreement (D), and the scatter index (SI). The explanations for the statistical measures appear in Table 2. These criteria are widely reported in the literature (Kisi 2014; Samaras et al. 2014; Celestin et al. 2020).

The R^2 coefficient, acquired by the least squared regression analysis, is a commonly used correlation measure. For the absolute and/or relative errors' estimation, RMSE, APE, and MBE indices were also evaluated. The descriptive index of agreement (D) was used for the correlation between the equations, expressing the degree to which an equation's predictions are error-free (Willmott 1982). According to Li et al. (2013), the range of SI for the accuracy of the models is excellent (SI < 0.1), good (0.1 < SI < 0.2), fair (0.2 < SI < 0.3), and poor (SI > 0.3).

In Eqs. (37) to (42), ${ET_{ref_i}}^{PM_{FAO56}}$ and $ET_{ref_i}^{\mathrm{model}}$ are the ET_{ref} based on PM-FAO_{56}, and modeled ET_{ref}, $\overline{ET}_{ref}^{PM_{FAO56}}$ and $\overline{ET}_{ref}^{\mathrm{model}}$ are the mean values of ET_{ref} based on PM-FAO_{56} and modeled ET_{ref} and N is the number of data sets.

2.4 Empirical equation calibration

The basis of empirical equations used in estimating ET_{ref} is the regression relationship between the ET_{ref} equation as a dependent variable and meteorological parameters as independent variables. In the process of developing each of the empirical equations, one of two modifications may be made, either a change in meteorological parameters or a change in the coefficients of the equation. In this study, modification (optimization) of constant coefficients in empirical equations is the basis for increasing the accuracy of ET_{ref} estimation in different climates. The objective function of that change has been to minimize the RMSE error criterion by optimizing the constant coefficients of the equations as decision variables. For instance, in the HASA equation, the two coefficients a and b in Eq. (43) are optimized to minimize the amount of error between the estimated ET_{ref} and the PM-FAO_{56}.

$$ET_{ref} = \left[a \times R_a (T_{mean} + 17.8)(T_{\max} - T_{\min})^b\right]/\lambda \quad (43)$$

The accuracy of empirical equations in estimating ET_{ref} before and after calibration was evaluated using error evaluation criteria separately for various empirical equations (temperature-based, solar radiation–based, and mass transfer–based) and for very dry, dry, semidry, and humid climates.

Table 2 The characteristics of evaluation performance criteria used in the study

Code	Criteria	Equation	References
(37)	Coefficient of determination (R^2)	$R^2 = \left[\frac{\sum_N^{i=1}\left(ET_{ref_i}^{PM_{FAO56}} - \overline{ET}_{ref}^{PM_{FAO56}}\right)\left(ET_{ref_i}^{\mathrm{model}} - \overline{ET}_{ref}^{\mathrm{model}}\right)}{\sqrt{\left[\sum_{i=1}^N\left(ET_{ref_i}^{PM_{FAO56}} - \overline{ET}_{ref}^{PM_{FAO56}}\right)^2\right]\left[\sum_{i=1}^N\left(ET_{ref_i}^{\mathrm{model}} - \overline{ET}_{ref}^{\mathrm{model}}\right)^2\right]}}\right]^2$	Ma and Iqbal (1984)
(38)	Root mean square error (RMSE)	$RMSE = \sqrt{\frac{1}{N}\sum_{i=1}^N\left(ET_{ref_i}^{\mathrm{model}} - ET_{ref_i}^{PM_{F56}}\right)^2}$	Ma and Iqbal (1984)
(39)	Average percentage error (APE)	$APE = \frac{\sum_{i=1}^N\left\lvert ET_{ref_i}^{PM_{FAO56}} - ET_{ref_i}^{\mathrm{model}}\right\rvert}{\sum_{i=1}^N ET_{ref_i}^{PM_{FAO56}}} \times 100\%$	Behar et al. (2015)
(40)	Mean bias error (MBE)	$MBE = \frac{1}{N}\sum_N^{i=1}\left(ET_{ref_i}^{\mathrm{model}} - ET_{ref_i}^{PM_{FAO56}}\right)$	Ferreira and da Cunha (2020)
(41)	Index of agreement (D)	$D = 1 - \frac{\sum_N^{i=1}\left(ET_{ref_i}^{\mathrm{model}} - ET_{ref_i}^{PM_{FAO56}}\right)^2}{\sum_N^{i=1}\left(\left\lvert ET_{ref_i}^{\mathrm{model}} - \overline{ET}_{ref}^{PM_{FAO56}}\right\rvert + \left\lvert ET_{ref_i}^{\mathrm{model}} - \overline{ET}_{ref}^{PM_{FAO56}}\right\rvert\right)^2}$	Seifi and Riahi-Madvar (2019)
(42)	Scatter index (SI)	$SI = \frac{RMSE}{\overline{ET}_{ref}^{PM_{FAO56}}}$	Li et al. (2013)

Table 3 The original and calibrated values of R^2 and RMSE for empirical ET_{ref} equations in different climates of Iran

Equation		Very dry R^2 Ori.	Very dry R^2 Cal.	Very dry RMSE Ori.	Very dry RMSE Cal.	Dry R^2 Ori.	Dry R^2 Cal.	Dry RMSE Ori.	Dry RMSE Cal.	Semidry R^2 Ori.	Semidry R^2 Cal.	Semidry RMSE Ori.	Semidry RMSE Cal.	Humid R^2 Ori.	Humid R^2 Cal.	Humid RMSE Ori.	Humid RMSE Cal.
Temperature-based	HASA	0.54	0.77	83.38	43.99	0.44	0.70	82.41	37.67	0.32	0.59	79.99	34.41	0.42	0.67	70.15	37.23
	TRAJ	0.54	0.80	80.48	39.18	0.44	0.69	77.59	40.29	0.28	0.60	77.87	35.63	0.40	0.68	80.81	38.80
	TATA1	0.49	0.78	78.73	40.66	0.34	0.68	76.75	39.46	0.20	0.59	62.12	32.56	0.32	0.68	73.03	34.94
	TATA2	0.53	0.76	73.20	39.97	0.38	0.68	83.42	40.71	0.36	0.61	74.34	34.37	0.39	0.68	85.12	34.05
	DRAL1	0.50	0.75	70.68	38.78	0.41	0.73	82.01	36.40	0.36	0.62	70.43	32.65	0.40	0.70	85.27	37.61
	DRAL2	0.48	0.79	84.88	43.97	0.36	0.67	72.66	41.21	0.23	0.55	69.24	36.91	0.32	0.66	78.29	35.49
	BERT	0.52	0.79	83.42	36.88	0.42	0.70	77.57	37.81	0.27	0.66	82.50	31.16	0.39	0.70	67.92	30.58
	DORJ	0.53	0.78	90.22	41.95	0.40	0.69	82.48	39.61	0.26	0.62	74.14	33.37	0.38	0.69	70.24	32.08
	BARO	0.71	0.82	65.05	32.79	0.63	0.73	74.69	42.12	0.46	0.65	60.25	30.34	0.59	0.71	73.35	35.29
	AHOO1	0.56	0.79	72.75	40.43	0.42	0.72	80.13	38.94	0.31	0.62	73.51	33.57	0.41	0.70	73.69	32.84
	AHOO2	0.54	0.76	65.58	38.36	0.39	0.71	81.70	38.74	0.28	0.59	76.76	39.36	0.39	0.68	67.84	36.71
Solar radiation–based	MAKK	0.43	0.77	69.82	32.77	0.42	0.71	66.56	37.34	0.24	0.52	56.31	36.24	0.37	0.66	75.22	33.71
	PRTA	0.49	0.83	73.92	37.98	0.41	0.72	74.28	38.43	0.38	0.63	65.67	35.22	0.42	0.71	83.72	35.38
	JEHA	0.50	0.78	71.27	32.39	0.42	0.69	65.92	37.25	0.42	0.60	53.08	34.23	0.44	0.68	66.77	41.86
	HARG	0.60	0.79	71.45	37.54	0.47	0.70	82.83	41.01	0.35	0.57	77.92	36.34	0.45	0.68	69.82	34.75
	ABTE1	0.54	0.82	80.25	33.30	0.43	0.69	71.60	38.40	0.43	0.58	77.11	38.25	0.44	0.67	85.44	37.09
	ABTE2	0.51	0.77	78.60	35.59	0.44	0.74	85.22	34.90	0.35	0.59	75.66	35.93	0.42	0.69	82.89	38.51
	IRMA1	0.53	0.77	88.50	38.48	0.44	0.74	77.14	37.32	0.34	0.60	79.41	37.52	0.43	0.70	71.64	35.71
	IRMA2	0.55	0.80	67.51	32.29	0.45	0.71	77.56	38.52	0.35	0.61	77.79	41.90	0.43	0.69	69.01	38.63
	TATA3	0.51	0.78	79.88	38.96	0.44	0.72	71.85	39.05	0.36	0.63	78.98	34.36	0.42	0.70	74.70	35.57
	TATA4	0.45	0.77	82.61	39.48	0.42	0.70	78.05	54.78	0.28	0.60	76.11	35.62	0.38	0.68	79.58	40.30
	OUDI	0.51	0.84	70.61	33.13	0.45	0.72	73.87	61.40	0.36	0.59	70.91	38.62	0.42	0.70	86.26	33.80
Mass transfer–based	DALT	0.56	0.82	66.53	31.11	0.59	0.71	76.56	53.83	0.36	0.65	66.21	36.12	0.51	0.71	75.23	34.40
	MEYE	0.67	0.80	80.83	36.93	0.60	0.71	72.02	56.87	0.44	0.64	61.90	33.51	0.55	0.70	70.29	35.10
	ROHW	0.68	0.76	72.71	38.88	0.58	0.73	74.26	52.57	0.31	0.63	70.95	38.54	0.50	0.70	67.41	36.73
	ALBR	0.63	0.79	64.30	39.43	0.48	0.72	71.79	65.94	0.30	0.56	65.62	47.00	0.44	0.68	72.52	31.83
	WMO	0.67	0.81	68.91	34.10	0.58	0.74	72.37	53.26	0.27	0.63	70.84	36.75	0.48	0.71	69.69	38.68
	TRAB	0.69	0.82	71.94	36.76	0.62	0.71	73.93	36.43	0.31	0.63	70.26	36.38	0.51	0.71	81.45	38.86
	BRWE	0.56	0.86	87.93	33.20	0.49	0.73	80.31	35.17	0.33	0.64	78.86	38.63	0.44	0.72	77.47	35.62
	MAHR	0.61	0.83	71.85	33.01	0.64	0.75	71.92	35.79	0.32	0.62	75.02	35.87	0.51	0.71	75.93	37.77
	PENM	0.74	0.85	54.17	27.87	0.70	0.79	53.13	31.83	0.53	0.71	46.46	29.38	0.64	0.77	56.72	31.71
	ROMA	0.50	0.76	59.22	30.93	0.45	0.73	69.14	36.09	0.42	0.61	49.03	30.99	0.46	0.70	49.20	30.14

3 Results

3.1 Accuracy evaluation of empirical equations

To assess the 32 empirical equations for temperature-based, solar radiation–based, and mass transfer–based models in different climates, meteorological datasets from 1990 to 2019 were evaluated. Table 3 shows the values of R^2 and RMSE for original and calibrated empirical equations based on temperature, solar radiation, and mass transfer methods in different climates. According to the results of the best values of R^2 and RMSE in the temperature-based BARO equation for very dry (0.71 and 65.05), dry (0.63 and 74.69), semidry (0.46 and 60.25), and humid (0.59 and 73.35) climates observed in original BARO equation. These values after calibration were 0.82 and 32.79 in very dry climate, 0.73 and 42.12 in dry climate, 0.65 and 30.34 in semidry climate, and 0.71 and 35.29 in humid climate. The DRAL1 equation in dry climate (0.73 and 36.4), and BERT equation in semidry (0.66 and 31.16) and humid climates (0.7 and 30.58) had acceptable results (Table 3).

For solar radiation–based methods, the maximum R^2 in very dry, dry, and humid climates derived by the original HARG equation was 0.6, 0.47, and 0.45, respectively, but the best RMSE in very dry climate obtained by the original IRMA1 equation was 67.51, and in dry and humid climates as obtained by the original JEHA equation was 65.92 and 66.77, respectively. The result for calibrated equations showed that in very dry (R^2 = 0.84 and RMSE = 33.13), dry (R^2 = 0.74 and RMSE = 34.9), and semidry (R^2 = 0.63 and RMSE = 34.36) climates, the OUDI, ABTE2, and TATA3 equations yielded reliable estimates. In the humid climate, calibrated PRTA and MAKK equations showed the maximum R^2 = 0.71 and the minimum RMSE = 33.71 (Table 3).

The results from mass transfer–based methods showed that the values of R^2 for the original PEMN equation in very dry, dry, semidry, and humid climates were acceptable (0.74, 0.7, 0.53, and 0.64, respectively). The values of RMSE for the

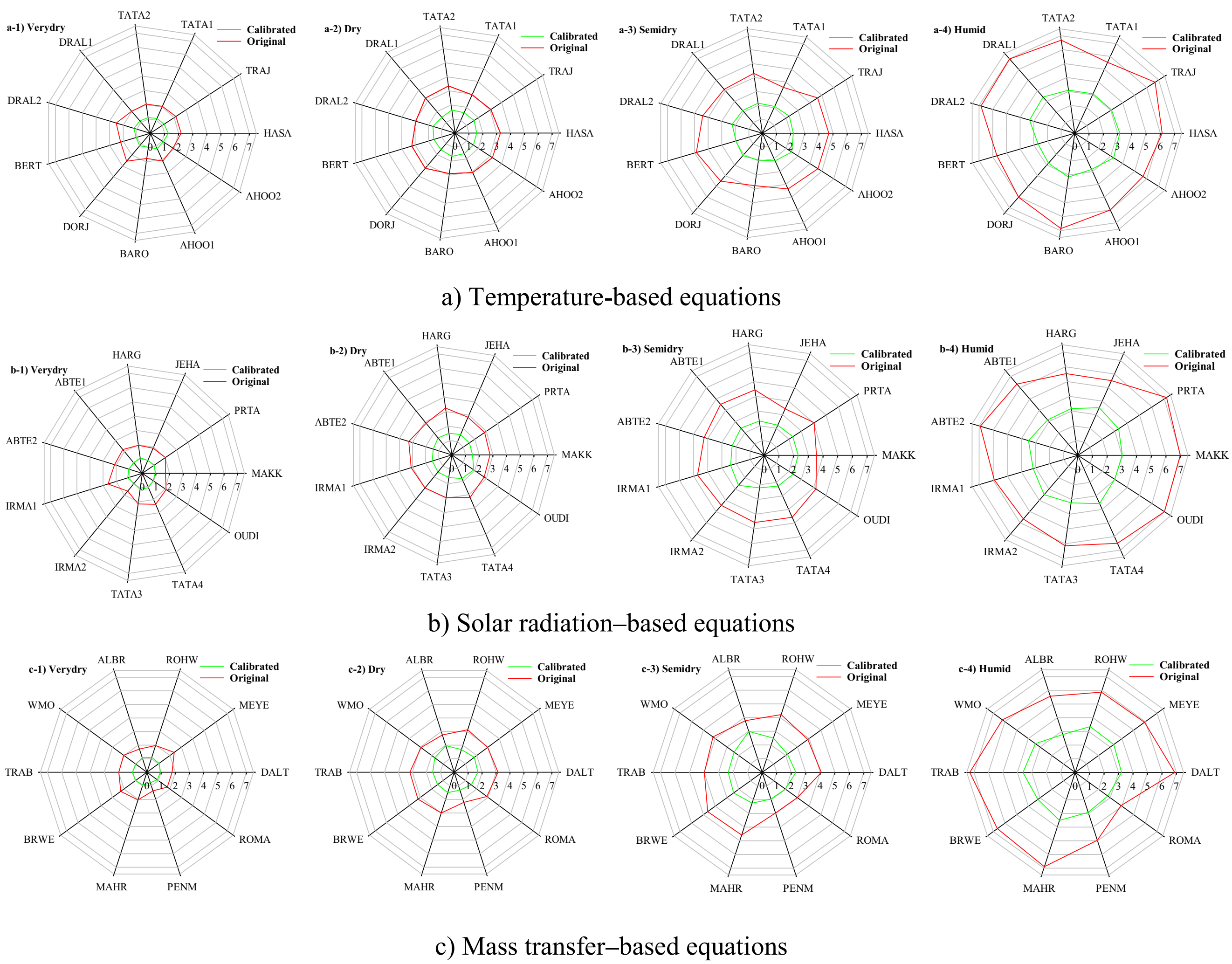

Fig. 3 The APE performance of original and calibrated empirical equations in different climates. **(a)** Temperature-based equations. (**b**) Solar radiation–based equations. (**c**) Mass transfer–based equations

original PENM equation were reported as 54.17 for very dry, 53.13 for dry, and 46.46 for semidry climates, but the best value of RMSE for humid climates, 49.2, was obtained by the original ROMA equation.

The results from mass transfer–based methods showed that the values of R^2 for the calibrated PEMN equation in very dry, dry, semidry, and humid climates were acceptable (0.85, 0.79, 0.71, and 0.77, respectively). The values of RMSE for the calibrated PEMN equation were 27.87 for very dry, 31.83 for dry, and 29.38 for semidry climates, but the best value of RMSE for humid climates, 30.14, was obtained by the calibrated ROMA equation (Table 3).

Radar charts in Fig. 3 compare the APE values of the $ET_{ref}^{PM_{FAO56}}$ and the estimated ET_{ref} using the original and calibrated empirical equations for temperature-based, solar radiation–based, and mass transfer–based methods from 1990 to 2019. Based on the results of APE plots, calibration greatly improved the performance of all empirical equations in all investigated climates compared with the original empirical equations. After calibration, APE values are closer to zero.

A reduction in values of APE for the calibrated empirical equations was found in very dry, dry, semidry, and humid climates in temperature-based (1, 1.5, 2.2, and 3.2%), solar radiation–based (1, 1.4, 1.9, and 3.1%), and mass transfer–based (1, 1.3, 1.6, and 2.8%) methods when compared to the original equations (Fig. 3). This indicates the great effect calibration has relative to other empirical equations on increasing the accuracy of temperature-based methods. This increase confirms the accuracy of calibrated empirical equations in estimating ET_{ref} in humid climate. At the same time, the accuracy of ET_{ref} estimation for all empirical equations decreased from very dry to humid climates, indicating that the process of ET_{ref} estimation in humid climate is more complex due to its greater dependence on multiple climatic parameters.

3.2 Bias error evaluation of empirical equations

Figure 4 shows a decrease in MBE for calibrated empirical equations compared to the original empirical equations. This error reduction is evident in all types of equations and in all climates. Figure 4(a) shows the overestimation of most

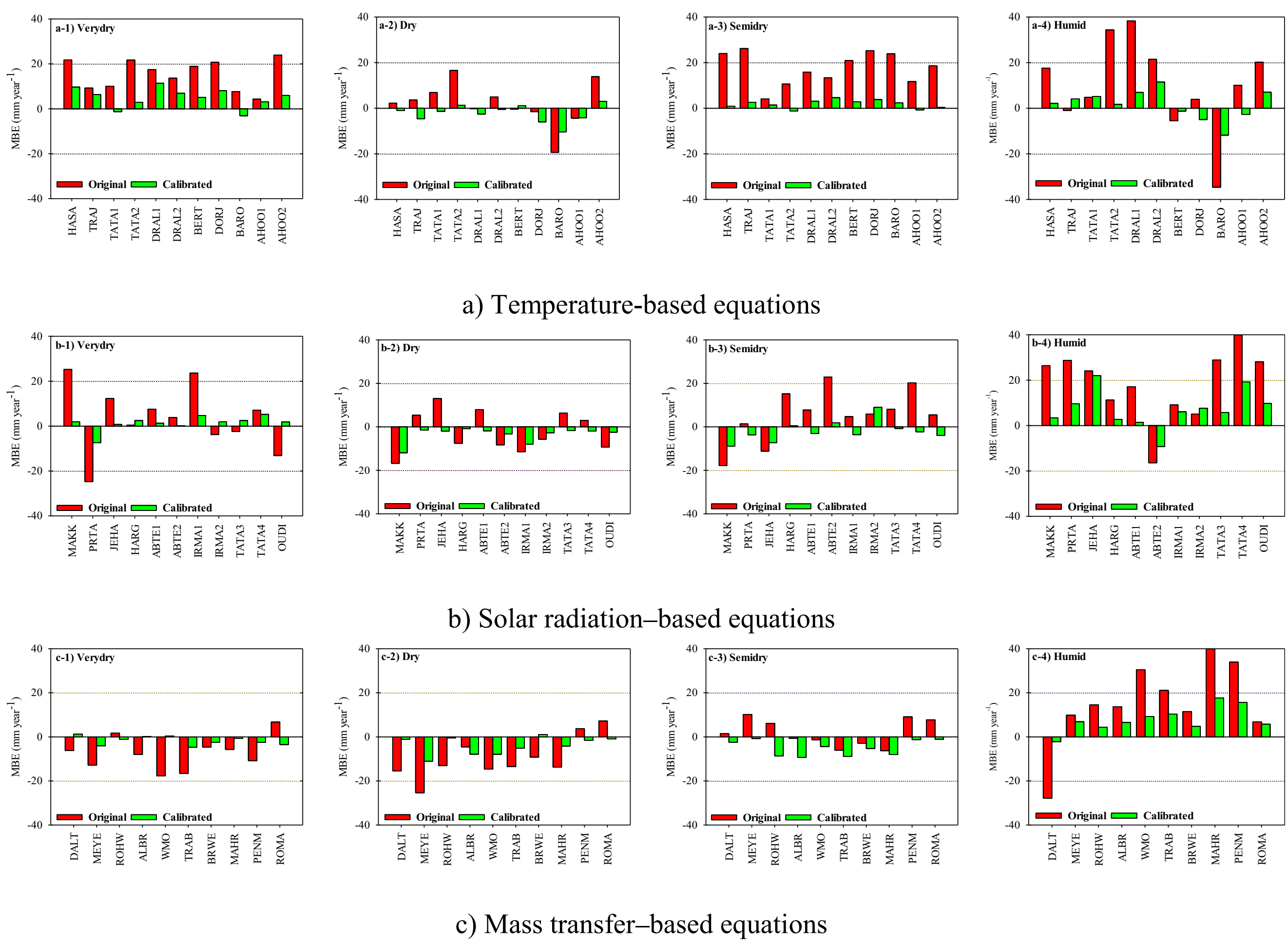

Fig. 4. The MBE performance of original and calibrated empirical equations in different climates. (**a**) Temperature-based equations. (**b**) Solar radiation–based equations. (**c**) Mass transfer–based equations

empirical temperature-based methods in very dry, semidry, and humid climates. The highest accuracy of empirical equations for temperature-based and solar radiation–based methods for estimating ET_{ref} in dry climate (Fig. 4(a-2) and (b-2)) is obtained when the MBE in this climate for all empirical equations is less than 20 mm year^{-1}. Figure 4(c) shows the overestimation of ET_{ref} values for mass transfer–based empirical equations in humid climate and underestimation in very dry, dry, and semidry climates. The highest accuracy of MBE is acquired by mass transfer–based methods in semidry climate.

For temperature-based equations, the negative MBE values are observed for calibrated TATA1 and BARO equations in very dry climate, the original BARO and AHOO1 equations and calibrated HASA, TRAJ, TATA1, DRAL1, DORJ, BARO, and AHOO1 equations in dry climate, calibrated TATA2 and AHOO1 equations in semidry climate and, finally, BERT, DORJ, BARO, and AHOO1 calibrated equations in humid climate, indicating that the tendency of these equations is to underestimate ET_{ref} (Fig. 4(a)). The MBE values for most original and calibrated equations were overestimated in very dry (Fig. 4(a-1)) and dry (Fig. 4(a-3)) climates. Also, it is noteworthy that the highest overestimation and underestimation were observed in humid climate, which was reported in MAHR (39.9 mm year^{-1}) and BARO (−34.3 mm year^{-1}) original equations, respectively (Fig. 4(a-4), 4(c-4)). The overestimation of the in original equations varied from 25.27 mm year^{-1} to 26.15 mm year^{-1} in very dry and semidry climates, respectively. The overestimation of the temperature-based equations was found by Trajkovic (2007) and Landeras et al. (2008). Furthermore, according to Temesgen et al. (2005), higher wind speed combined with lower humidity resulted in lower values of temperature-based equations compared to PM-FAO_{56}, especially in drier climates.

For solar radiation–based methods, the negative MBE values are observed for PRTA, IRMA2, TATA3, and OUDI original equations and PRTA calibrated equation in very dry climate, and ABTE2 original and calibrated equations in humid climate. Also, most equations in very dry, dry, and semidry climates showed a good response to calibration. In humid climate, due to the influence of more factors on ET_{ref}, more fluctuations were observed. However, the calibrated MAKK, HARG, and ABTE1 equations showed better results in humid climate (Fig. 4(b-4)). Analyses by Trajkovic and Kolakovic (2009) showed the solar radiation–based equations had a tendency to overestimate ET_{ref} in humid climates of Serbia.

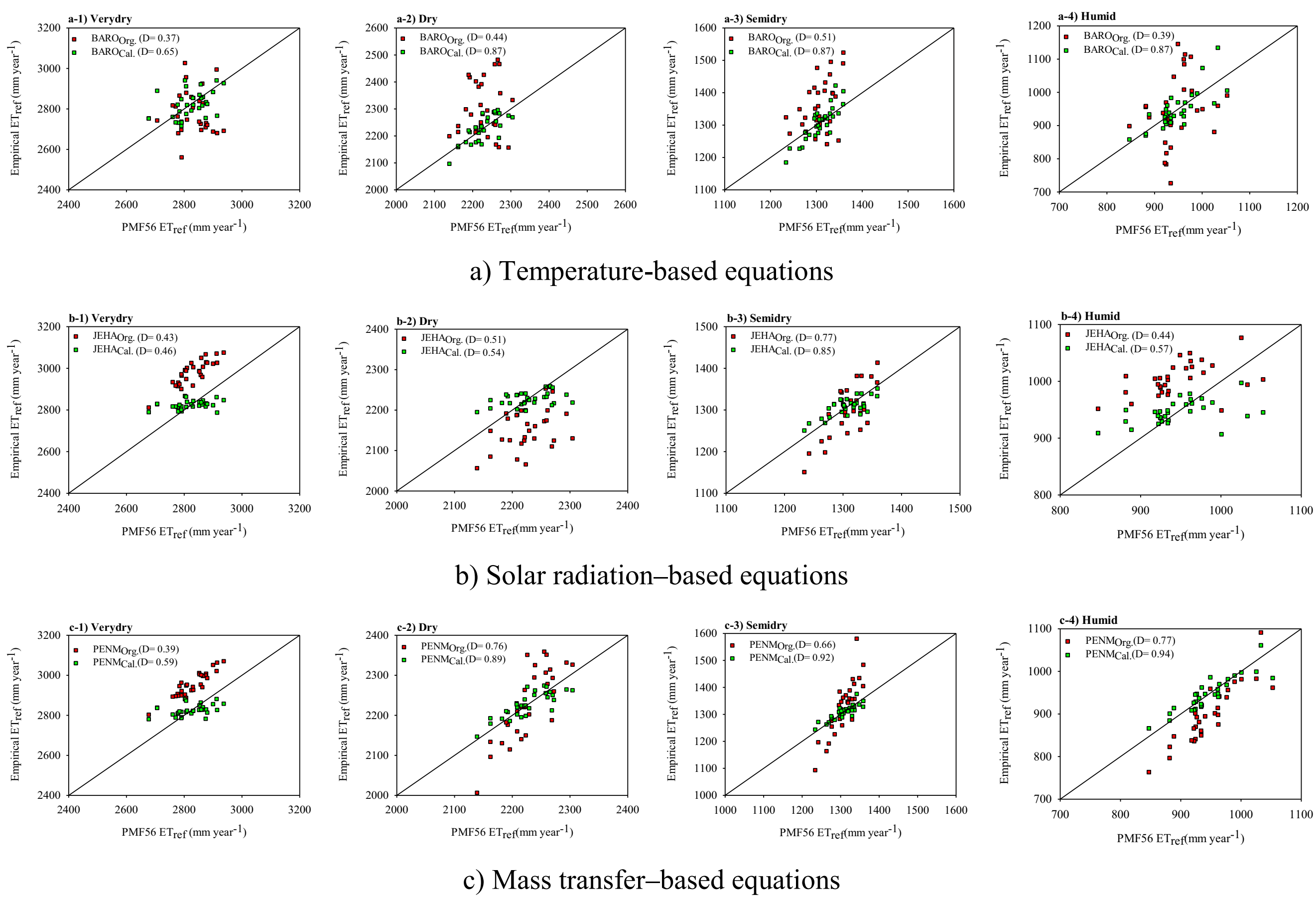

Fig. 5. The D performance of original and calibrated empirical equations in different climates. (**a**) Temperature-based equations. (**b**) Solar radiation–based equations. (**c**) Mass transfer–based equations

For mass transfer–based equations, most of the original and calibrated equations exhibited underestimation in very dry, dry, and semidry climates. According to the MBE values, the original and calibrated equations of ROHW in the very dry climate, PENM in the dry climate, DALT in the semidry climate, and ROMA in the humid climate showed better results (Fig. 4(c)). In general, the comparative results revealed that the mass transfer-based equations had the best performances among the ET_{ref} equations evaluated in very dry and semidry climates. Also, the temperature-based and solar radiation–based equations were the good equations for the dry climates (Fig. 4(a) and (b)).

3.3 Correlation between PM-FAO$_{56}$ and empirical equations

Based on the results presented in Table 3, the highest accuracy of empirical equations for temperature-based, solar radiation–based, and mass transfer–based methods of estimating ET_{ref} in different climates is determined by the BARO, JEHA, and PENM equations, respectively. Figure 5 shows the values of D for the best equations of temperature-based, solar radiation–based, and mass transfer–based methods in different climates. A better fit between the estimated ET_{ref} and *PM-FAO$_{56}$* appears in the calibrated empirical equations when compared to the original empirical equations in all empirical equations and climates.

The best fit between the *PM-FAO$_{56}$* and estimated ET_{ref} values is related to the calibrated PENM equation in humid climate and is equal to 0.94 (Fig. 5(c-4)). Generally, the best and worst fit between the *PM-FAO$_{56}$* and estimated ET_{ref} values were related to the mass transfer–based (Fig. 5(c)) and the solar radiation–based methods (Fig. 5(b)).

Figure 6 shows *PM-FAO$_{56}$* and estimated ET_{ref} values for the best empirical equations in different climates during 1990 to 2019. The estimated ET_{ref} values using the empirical equations after calibration are very close to the calculated ET_{ref} values. This can especially be seen in the calibrated PENM equation in semidry climate (Fig. 6(c-3)).

Figure 6 makes it clear that the calibrated techniques show better accuracy when compared to the original equations. For temperature-based equations, the best correlation was showed by calibrated BARO equation with R^2 0.82, 0.73, 0.65, and 0.71 in very dry, dry, semidry, and humid climates, respectively. This equation resulted in the highest D index, ranging from 0.65 in very dry climate to 0.87 in dry, semidry, and humid climates

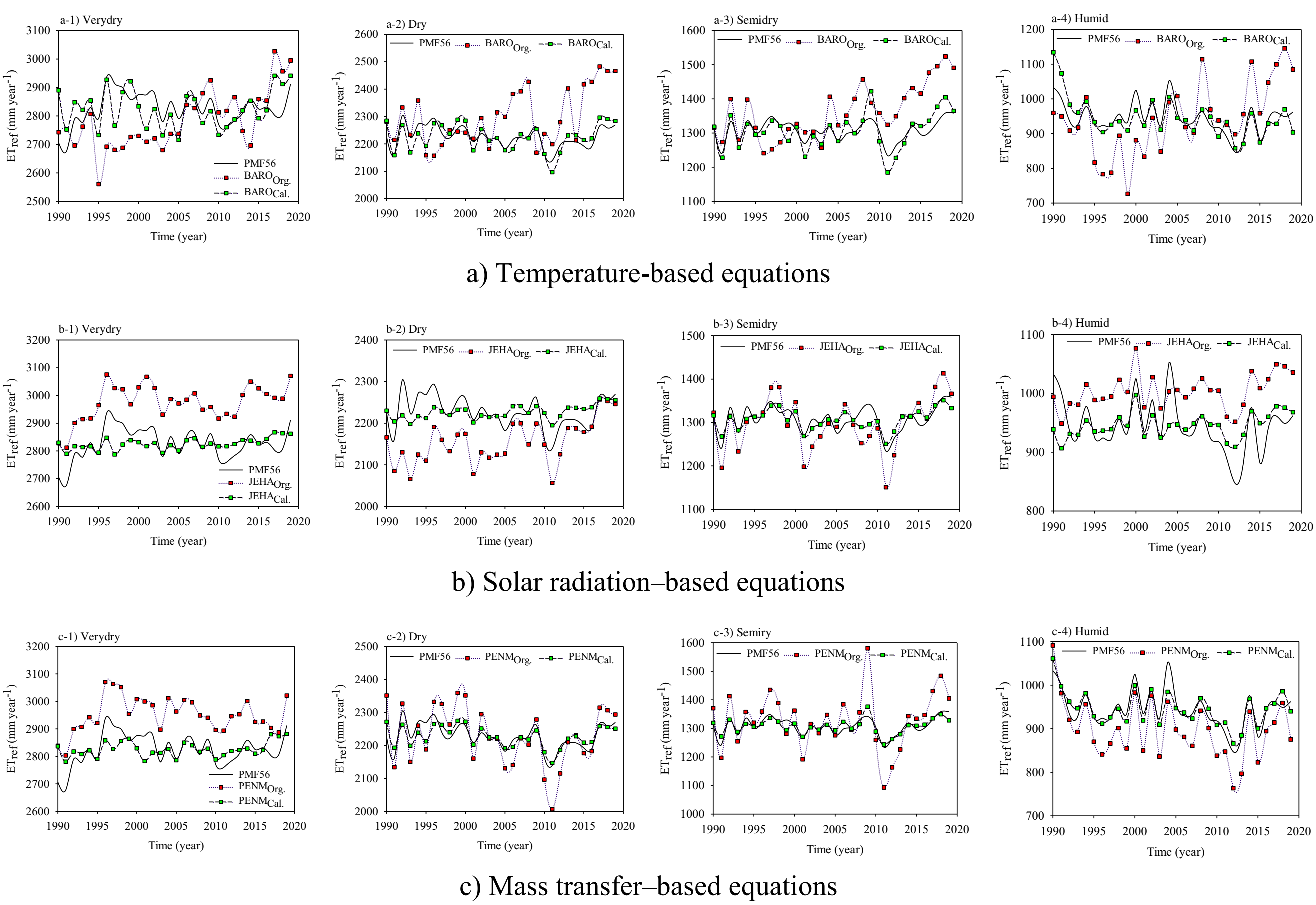

Fig. 6 The estimated ET_{ref} versus PM-FAO$_{56}$ values in different climates. (**a**) Temperature-based equations. (**b**) Solar radiation–based equations. (**c**) Mass transfer–based equations

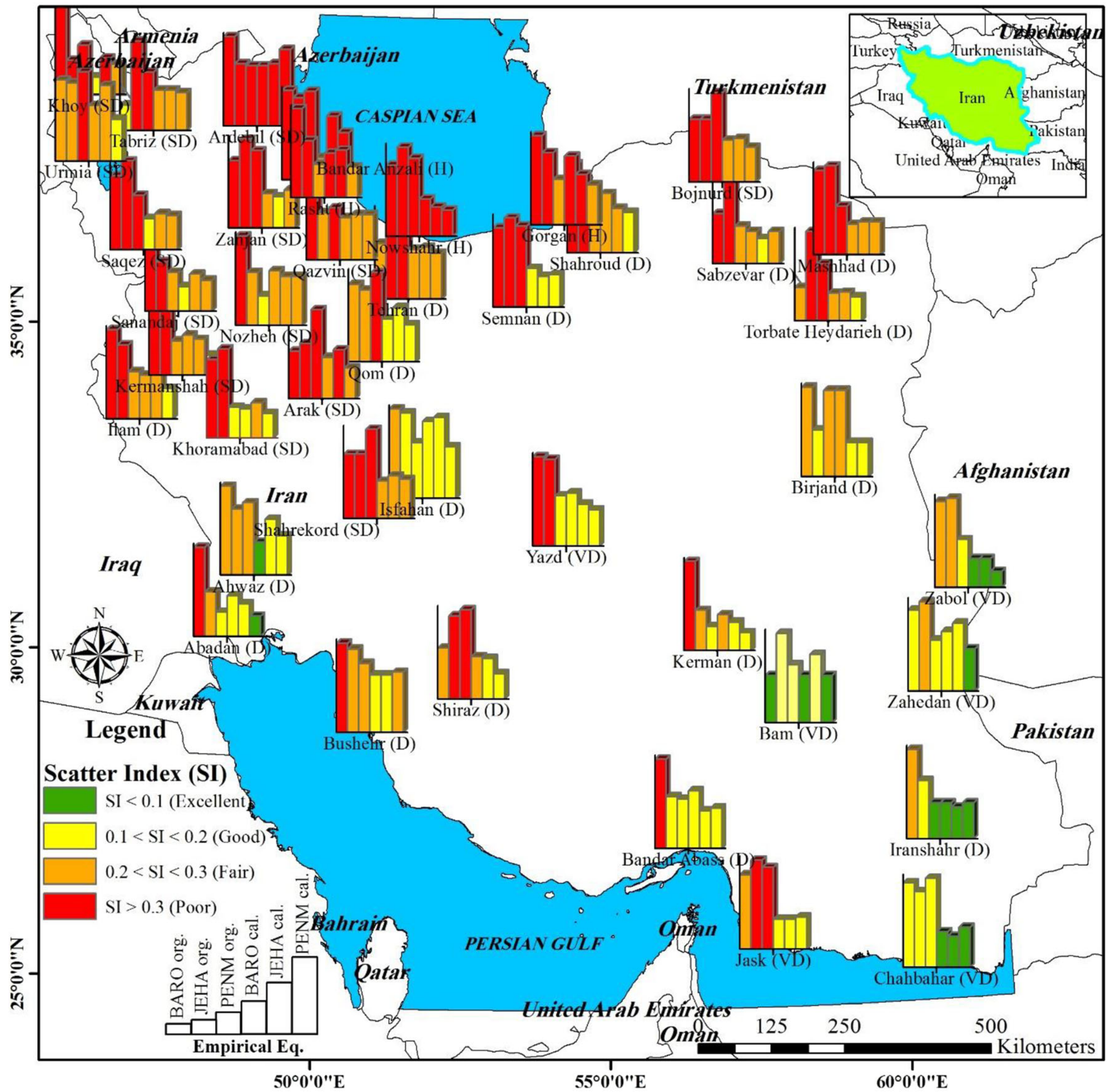

Fig. 7 SI map of the best empirical equations in different climates

(Fig. 5(a-1–4)). The results indicated a slight underestimation in ET_{ref} values for calibrated BARO equation in comparison to PM-FAO_{56} (Fig. 6(a-1–4)). The radiation-based equations overall performed better than the mass transfer equations, since a more important role is expected for R_s when estimating ET_{ref} in humid climates (Irmak et al. 2006). The calibrated JEHA equation exhibited the highest R^2 and lowest RMSE (Table 3). Additionally, this equation presented the D index from 0.46 in very dry climate to 0.85 in semidry climate (Fig. 5(b-1–4)). Therefore, it can be concluded that the JEHA equation of this class can be suitable for estimating of ET_{ref} values in surveyed climates (Fig. 6(b-1–4)). These results for JEHA are in contrast to Tabari et al. (2013), who surveyed in humid climates. Among the 10 empirical equations from mass transfer–based methods, the calibrated PEMN equation showed accurate ET_{ref} equal to 2826, 2227, 1308, and 946 mm year^{-1} in very dry, dry, semidry, and humid climates, respectively (during 1990 to 2019). Simultaneously, it displayed the highest correlation coefficient (R^2 = 0.85, 0.79, 0.71, and 0.77 in very dry, dry, semidry, and humid climates, respectively). On the other hand, this equation resulted in the highest D index ranging from 0.59 in very dry climate to 0.94 in humid climate (Fig. 5(c-1–4). Overall, the statistical indices of the mass transfer–based equations were reasonable in humid climate. Based on Valipour 2015), mass transfer–based equations cannot be suggested for use without calibration.

From the abovementioned, it can be concluded that the calibrated equations of BARO, JEHA, and PENM equations (as a good alternative for ET_{ref} estimations) have similar performance and they are recommended for use in different climates of Iran (Fig. 6).

3.4 SI map

Figure 7 shows that calibration at stations with very dry climate, such as Zabol, Zahedan, Bam, Iranshahr, and Chabahar stations, had a greater effect on the accuracy of ET_{ref} estimation based on the SI value in the excellent class (SI < 0.1). The highest amount of error in the SI index is related to stations with humid climates, such as Rasht and Nowshahr. This is due to the complexity of the ET_{ref} process in humid climate.

The SI map demonstrates that the original temperature, radiation, and mass transfer–based equations generally did not have excellent class (SI < 0.1), except BARO and PENM equations in Bam and Iranshahr stations, respectively. In general, the results of the present study confirmed that temperature-based equation had the more accuracy than solar radiation and mass transfer–based equations. Similar results were also reported by Farzanpour et al. (2019). Their results cleared that the temperature- and radiation-based equations generally have had similar SI values, giving more accurate simulations than the mass transfer–based equations. This might show the importance of temperature parameters on ET_{ref} estimating in the very dry and dry stations, as well as its superiority to the solar radiation-based. The impact of input climatic parameters seems to be very low as the mass transfer–based equations gave the undesirable results in these climates. However, this situation should be used with cautiousness because a comprehensive study should be conducted to determinate the portion of each parameter on the empirical ET_{ref} magnitudes, which is beyond the scope of this research.

4 Conclusion

The accurate estimation of ET_{ref} by empirical equations can be helpful for water resources management, crops' water demand, and irrigation scheduling. This study attempted to investigate and calibrate 32 empirical equations classified in three categories (temperature-based, solar radiation–based, and mass transfer–based) in main climates (very dry, dry, semidry, and humid) of Iran. The results show that most of the calibrated empirical equations had good accuracy in estimating ET_{ref} in all studied climates. However, the accuracy of the ET_{ref} estimate before and after calibration depended on the classification of the equation in the type and number of input data and the type of climate under study. In other words, each climatic region has its own superior empirical equation. Also, with the complexity of climatic variables, the accuracy of various empirical equations is associated with change.

According to the results of the best values of R^2 and RMSE in the temperature-based BARO equation for very dry (0.82 and 32.79), dry (0.73 and 42.12), semidry (0.65 and 30.34), and humid (0.71 and 35.29), climates were observed in the calibrated BARO equation. Also, the calibrated JEHA equation showed reliable estimates in very dry (R^2 = 0.78 and RMSE = 32.39), dry (R^2 = 0.69 and RMSE = 37.25), semidry (R^2 = 0.60 and RMSE = 34.23), and humid (R^2 = 0.68 and RMSE = 41.86) climates. Finally, the best values of R^2 and RMSE were reported for the calibrated PENM equation in very dry (0.85 and 27.87), dry (0.79 and 31.83), semidry (0.71 and 29.38), and humid (0.77 and 31.71) climates, respectively. The results of APE, MBE, and D criteria show that the accuracy of the empirical equations after calibration increased significantly when compared to their original values. At the same time, the results of SI criterion and the effect of factors such as high relative humidity and the balance between air temperature and rainfall mean that the estimation of ET_{ref} is more complex. Considering the dependence of the ET_{ref} process on fewer meteorological parameters, we can conclude that in very dry climates the empirical equations before and after calibration are more accurate.

Considering the limitations associated with the availability and reliability of the climatological data, especially in developing countries, the good performance of empirical models must be emphasized, since they deal with a very simple equation. Further studies are needed in order to evaluate the performance of the calibrated equations in other areas in the world with different climates. Also, evaluation is needed for the performance of the empirical equations on a different time scale (daily). Therefore, more studies might use empirical equations and stations as well as other calibration scenarios for assessing these results in various climates.

Acknowledgments We thank the Agricultural Experiment Station of Arak University and Ms. Sunny Skies.

Availability of data and material All data used in this article have been prepared from the Meteorological Organization of Iran and, after validation, have been used. In this study, meteorological information was used that lacked outdated data.

Code availability The software used in this research will be available (by the corresponding author), upon reasonable request.

Authors' contributions All authors contributed to the study conception and design. Material preparation, data collection, and analysis were performed by Saeed Sharafi and Mehdi Mohammadi Ghaleni. The first draft of the manuscript was written by Saeed Sharafi, and all authors commented on previous versions of the manuscript. All authors read and approved the final manuscript.

Funding This research was funded by the Agricultural Experiment Station of Arak University, Iran.

Declarations

Ethics approval We confirm that we have given due consideration to the protection of intellectual property associated with this work and that there are no impediments to publication, including the timing of publication, with respect to intellectual property.

Consent to participate Conceptualization, methodology, technical investigation, writing (original draft preparation), supervision: S.S. Software validation: M.M.G. All authors have read and agreed to the published version of the manuscript.

Consent for publication We confirm that intellectual property associated with this work belongs to the *Journal of Theoretical and Applied Climatology*.

Conflict of interest The authors declare no conflict of interest.

References

Abtew W (1996) Evapotranspiration measurements and modeling for three wetland systems in South Florida 1 JAWRA. J Am Water Resour Assoc 32:465–473

Ahooghalandari M, Khiadani M, Jahromi ME (2016) Developing equations for estimating reference evapotranspiration in Australia. Water Resour Manag 30:3815–3828

Ahooghalandari M, Khiadani M, Jahromi ME (2017) Calibration of Valiantzas' reference evapotranspiration equations for the Pilbara region. Western Australia Theoretical and applied climatology 128:845–856

Albrecht F (1950) Die methoden zur bestimmung der verdunstung der natürlichen erdoberfläche Archiv für Meteorologie. Geophysik und Bioklimatologie, Serie B 2:1–38

Allen RG, Pereira LS, Raes D, Smith M (1998) Crop evapotranspiration-guidelines for computing crop water requirements-FAO Irrigation and drainage paper 56 FAO Rome 300(9):D05109

Allen RG et al (2006) A recommendation on standardized surface resistance for hourly calculation of reference ETo by the FAO56 Penman-Monteith method. Agric Water Manag 81:1–22

Baier W, Robertson GW (1965) Estimation of latent evaporation from simple weather observations Canadian. Journal of plant science 45: 276–284

Behar O, Khellaf A, Mohammedi K (2015) Comparison of solar radiation models and their validation under Algerian climate–The case of direct irradiance. Energy Convers Manag 98:236–251

Berti A, Tardivo G, Chiaudani A, Rech F, Borin M (2014) Assessing reference evapotranspiration by the Hargreaves method in North-Eastern Italy. Agric Water Manag 140:20–25

Bourletsikas A, Argyrokastritis I, Proutsos N (2018) Comparative evaluation of 24 reference evapotranspiration equations applied on an evergreen broadleaved forest. Hydrol Res 49(4):1028–1041

Brockamp B, Wenner H (1963) Verdunstungsmessungen auf den Steiner see bei münster Dt Gewässerkundl Mitt 7:149-154

Celestin S, Qi F, Li R, Yu T, Cheng W (2020) Evaluation of 32 simple equations against the Penman–Monteith method to estimate the reference evapotranspiration in the Hexi Corridor. Northwest China Water 12:2772

Dalton J (1802) Experimental essays on the constitution of mixed gases. Manchester Literary and Philosophical Society Memo 5:535–602

Dorji U, Olesen JE, Seidenkrantz MS (2016) Water balance in the complex mountainous terrain of Bhutan and linkages to land use. Journal of Hydrology: Regional Studies 7:55–68

dos Santos Farias DB, Althoff D, Rodrigues LN, Filgueiras R (2020) Performance evaluation of numerical and machine learning methods in estimating reference evapotranspiration in a Brazilian agricultural frontier. Theor Appl Climatol 142:1481–1492. https://doi.org/10.1007/s00704-020-03380-4

Droogers P, Allen RG (2002) Estimating reference evapotranspiration under inaccurate data conditions. Irrig Drain Syst 16:33–45

Farzanpour H, Shiri J, Sadraddini AA, Trajkovic S (2019) Global comparison of 20 reference evapotranspiration equations in a semi-arid region of. Iran Hydrology Journal 50(1):282–300. https://doi.org/10.2166/nh.2018.174

Ferreira LB, da Cunha FF (2020) New approach to estimate daily reference evapotranspiration based on hourly temperature and relative humidity using machine learning and deep learning. Agric Water Manag 234:106113

Ferreira LB, da Cunha FF, de Oliveira RA, Fernandes Filho EI (2019) Estimation of reference evapotranspiration in Brazil with limited meteorological data using ANN and SVM–a new approach. J Hydrol 572:556–570

Gafurov Z, Eltazarov S, Akramov B, Yuldashev T, Djumaboev K, Anarbekov O (2018) Modifying hargreaves-samani equation for estimating reference evapotranspiration in dryland regions of Amudarya River Basin Agricultural Sciences 9:1354

Gao F, Feng G, Ouyang Y, Wang H, Fisher D, Adeli A, Jenkins J (2017) Evaluation of reference evapotranspiration methods in arid, semiarid, and humid regions JAWRA. J Am Water Resour Assoc 53:791–808

Gholipoor M (2009) Evaluating the effect of crop residue on water relations of rainfed chickpeain maragheh, Iran, using simulation. International Meeting on Soil Fertility Land Management and Agroclimatology Turkey, p 737–748

Güçlü YS, Subyani AM, Şen Z (2017) Regional fuzzy chain model for evapotranspiration estimation. J Hydrol 544:233–241

Hargreaves GH (1975) Moisture availability and crop production. Trans ASAE 18(5):980–0984

Hargreaves GH, Samani ZA (1985) Reference crop evapotranspiration from temperature. Appl Eng Agric 1(2):96–99

Heydari MM, Heydari M (2014) Calibration of Hargreaves–Samani equation for estimating reference evapotranspiration in semiarid and arid regions. Arch Agron Soil Sci 60:695–713

Irmak S, Irmak A, Allen R, Jones J (2003) Solar and net radiation-based equations to estimate reference evapotranspiration in humid climates. J Irrig Drain Eng 129:336–347

Irmak S, Payero JO, Martin DL, Irmak A, Howell TA (2006) Sensitivity analyses and sensitivity coefficients of standardized daily. ASCE Penman-Monteith equation Journal of Irrigation and Drainage Engineering 132(6):564–578

Jensen ME, Haise HR (1963) Estimating evapotranspiration from solar radiation. J Irrig Drain Div 89:15–41

Kisi O (2014) Comparison of different empirical methods for estimating daily reference evapotranspiration in Mediterranean climate. J Irrig Drain Eng 40(1). https://doi.org/10.1061/(ASCE)IR.1943-4774.0000664 04013002

Landeras G, Ortiz-Barredo A, Lopez JJ (2008) Comparison of artificial neural network models and empirical and semi-empirical equations for daily reference evapotranspiration estimation in the Basque Country (Northern Spain) Agric. Water Manage 95:553–565

Li M-F, Tang X-P, Wu W, Liu H-B (2013) General models for estimating daily global solar radiation for different solar radiation zones in mainland China. Energy Convers Manag 70:139–148

Ma CCY, Iqbal M (1984) Statistical comparison of solar radiation correlations Monthly average global and diffuse radiation on horizontal surfaces. Solar Energy 33(2):143–148

Mahringer W (1970) Verdunstungsstudien am neusiedler See Archiv für Meteorologie. Geophysik und Bioklimatologie, Serie B 18:1–20

Makkink GF (1957) Testing the Penman formula by means of lysimeters. Journal of the Institution of Water Engineerrs 11:277–288

Mehdizadeh S, Saadatnejadgharahassanlou H, Behmanesh J (2017) Calibration of Hargreaves–Samani and Priestley–Taylor equations in estimating reference evapotranspiration in the Northwest of Iran. Arch Agron Soil Sci 63:942–955

Meyer A (1926) Über einige zusammenhänge zwischen klima und boden in Europa. ETH Zurich

Ndiaye PM, Bodian A, Diop L, Deme A, Dezetter A, Djaman K (2020) Evaluation and calibration of alternative methods for estimating reference evapotranspiration in the Senegal River Basin. Hydrology 7:24

Oudin L (2004) Recherche d'un modèle d'évapotranspiration potentielle pertinent comme entrée d'un modèle pluie-débit global (Doctoral dissertation, ENGREF (AgroParisTech))

Penman HL (1948) Natural evaporation from open water, bare soil and grass Proceedings of the Royal Society of London Series A. Mathematical and Physical Sciences 193(1032):120–145

Priestley CHB, Taylor RJ (1972) On the assessment of surface heat flux and evaporation using large-scale parameters. Mon Weather Rev 100:81–92

Rahimikhoob A, Behbahani MR, Fakheri J (2012) An evaluation of four reference evapotranspiration models in a subtropical climate. Water Resour Manag 26:2867–2881

Rohwer C (1931) Evaporation from free water surfaces. vol 271. US Department of Agriculture

Romanenko V (1961) Computation of the autumn soil moisture using a universal relationship for a large area Proc of Ukrainian. Hydrometeorological Research Institute 3:12–25

Saggi MK, Jain S (2019) Reference evapotranspiration estimation and modeling of the Punjab Northern India using deep learning. Comput Electron Agric 156:387–398

Samaras DA, Reif A, Theodoropoulos K (2014) Evaluation of radiation-based reference evapotranspiration models under different Mediterranean climates in Central Greece. Water Resour Manag 28:207–225

Seifi A, Riahi-Madvar H (2019) Improving one-dimensional pollution dispersion modeling in rivers using ANFIS and ANN-based GA optimized models. Environ Sci Pollut Res 26:867–885

Sharafi S, Ghaleni MM (2021) Evaluation of multivariate linear regression for reference evapotranspiration modeling in different climates of Iran. Theor Appl Climatol 143:1409–1423

Shiri J, Marti P, Karimi S, Landeras G (2019) Data splitting strategies for improving data driven models for reference evapotranspiration estimation among similar stations. Comput Electron Agric 162:70–81

Tanner CB, Sinclair TR (1983) Efficient water use in crop production: Research or re-search? Limitations to efficient water use in crop production, p 1–27

Tabari H, Talaee PH (2011) Local calibration of the Hargreaves and Priestley-Taylor equations for estimating reference evapotranspiration in arid and cold climates of Iran based on the Penman-Monteith model. J Hydrol Eng 16:837–845

Tabari H, Grismer M, Trajkovic S (2013) Comparative analysis of 31 reference evapotranspiration methods under humid conditions. Irrig Sci 31:107–117

Temesgen B, Eching S, Davidoff B, Frame K (2005) Comparison of some reference evapotranspiration equations for California. J Irrig Drain Eng ASCE 131:73–84

Trabert W (1896) Neue beobachtungen über verdampfungsgeschwindigkeiten. Meteorol Z 13:261–263

Trajkovic S (2007) Hargreaves versus Penman-Monteith under humid conditions. J Irrig Drain Eng 133:38–42

Trajkovic S, Kolakovic S (2009) Evaluation of reference evapotranspiration equations under humid conditions. Water Resour Manag 23:3057–3067

Valipour M (2015) Calibration of mass transfer-based models to predict reference crop evapotranspiration. Appl Water Sci 7(2):625–635

Willmott CJ (1982) Some comments on the evaluation of model performance. Bull Am Meteorol Soc 63(11):1309–1313

Yan S, Wu L, Fan J, Zhang F, Zou Y, Wu Y (2021) A novel hybrid WOA-XGB model for estimating daily reference evapotranspiration using local and external meteorological data: Applications in arid and humid regions of China. Agric Water Manag 244(1):106594